

Article

# A Layout Strategy for Distributed Barrage Jamming against Underwater Acoustic Sensor Networks

Mengchen Xiong<sup>1</sup>, Jie Zhuo<sup>1,\*</sup>, Yangze Dong<sup>2,\*</sup> and Xin Jing<sup>1</sup>

<sup>1</sup> School of Marine Science and Technology, Northwestern Polytechnical University, Xi'an 710072, China; xiongmcc@mail.nwpu.edu.cn (M.X.); 589jingx@mail.nwpu.edu.cn (X.J.)

<sup>2</sup> National Key Laboratory of Science and Technology on Underwater Acoustic Antagonizing, Shanghai 201108, China

\* Correspondence: jzhuo@nwpu.edu.cn (J.Z.); dongyangze@139.com (Y.D.)

Received: 9 March 2020; Accepted: 30 March 2020; Published: 3 April 2020



**Abstract:** Underwater acoustic sensor networks (UASNs) can effectively detect and track targets and therefore play an important role in underwater detection technology. To protect a target from being detected by UASNs, a distributed barrage jamming layout strategy is proposed, which considers the detection performance of UASNs as an indicator of the jamming performance. Since common indices of detection performance often involve specific signal processing methods, the Cramér–Rao bound (CRB) of multiple targets estimated by an UASN for distributed jammers is deduced in this paper, which is universal for all signal processing methods. The optimization model of the distributed jamming layout strategy is designed by maximizing the CRB to achieve the best jamming effect with limited jammers. A heuristic algorithm is used to solve this optimization model, and a numerical simulation shows that the optimal layout strategy for distributed jammers proposed in this paper achieves better performance than traditional jamming layout strategies. Considering the deviation of the position of the jammers from the ideal value due to the movement of water in a real marine environment, this paper also analyzes the jamming effects of strategies when there is error in the position of the jammers. The result proves the effectiveness and superiority of the proposed optimal layout strategy in an actual environment.

**Keywords:** distributed jamming technology; layout strategy; underwater acoustic sensor networks; Cramér–Rao bound

## 1. Introduction

In recent years, research on underwater acoustic sensor networks (UASNs) has received increasing attention. UASNs have great application prospects in the submarine field [1–4], including the monitoring of tsunamis and earthquakes and also military applications such as shore-based observation and target tracking. Compared with traditional detection systems, UASNs employ multiple sonar arrays working independently or collaboratively and can achieve direction measurements and also tracking and identification. Therefore, UASNs play an increasingly important role in the modern underwater detection field. With the development of related detection technologies, research on jamming strategies for UASNs is also attracting the attention of researchers [5]. The UASN jamming scenario usually includes several targets (marine vehicles such as ships and submarines) exposed in the UASN detection range. In order to avoid being detected by the UASN, the targets usually emit some noise jammers. Then the targets radiated signal received by the UASN is covered by jamming noise and the detection performance of the detector reduces. A well-designed jamming strategy can achieve the goal of protecting targets from being detected more effectively than other strategies and is an important research problem in underwater jamming technology.

Currently, the most common jamming method for underwater detection uses a single high-power jammer at a long distance. However, this approach cannot effectively jam all of the arrays in an UASN. A more flexible and effective jamming method should be applied in an underwater environment. Distributed jamming technology is a new type of jamming method [6] that uses many small low-cost jammers distributed near the receiving system that can jam multiple sensor arrays at the same time. Compared to traditional jamming methods, distributed jamming technology can achieve better results for UASNs.

Distributed jamming technology was first used to countermeasure radar systems. There are many studies on distributed jamming technology for radar systems with strong anti-jamming capabilities, such as multiple-input multiple-output (MIMO) radar [7–10] and networking radar [11]. However, most of these studies mainly focus on the power allocation of the jammers [7,8], without considering the influence of the locations of the distributed jammers. Due to the difference between the propagation medium and receiving equipment of the ground-based radio sensor networks and the underwater acoustic sensor networks [12], distributed jamming strategies in the radar field cannot be directly applied to UASNs. The receiver structures of UASNs are different from those of radar networks, so they have different detection methods, and the reflections of jamming effects against them are different. Related work in an underwater environment has only appeared in recent years. Jamming strategies for UASNs based on game theory were studied by Vadori and colleagues [13] and Xiao and co-workers [14]. In particular, the location of the jammer was studied by Vadori and colleagues [13], and the results showed that a jammer in some specific locations will have a stronger jamming effect on UASNs. However, research is limited to the case of a single jammer, and there is no description of the locations of distributed jammers.

In this paper, an optimal layout strategy for distributed jammers of UASNs is developed, which aims to minimize the target detection performance of the sensors by optimizing the location of the jammers, and thus protect the target from being attacked. Therefore, the detection performance of the UASNs can be applied as an evaluation index to evaluate the jamming performance. Since the same detection system using different signal processing methods will produce different estimation errors when estimating the target parameters, a more universal index should be considered. In a study by Zheng and colleagues [9], the Cramér–Rao bound (CRB) of MIMO radar was used to reflect the jamming performance, representing the minimum mean square error that the receiving system can achieve for an unbiased estimation of the target parameters. However, while the power allocation strategy of a single jammer was considered in their study [9], the distributed jammers and the effect of the jammers' location were not taken into consideration. In this paper, the CRB of an UASN is used to evaluate its detection accuracy. The larger the CRB, the larger the minimum estimation error that can be achieved by the receiver and the worse the parameter estimation performance of the receiver. Correspondingly, due to the effect of distributed jamming, the CRB of the receiver increases, which means that the jammers weaken the receiver's estimation performance for the target. Therefore, the CRB can be used as an evaluation index of the jamming effect. Based on this approach, an optimal distributed jamming layout strategy is proposed. By maximizing the CRB, the optimal locations of the distributed jammers can be obtained. In addition, since the calculation of the CRB is not limited to a specific signal processing method, the jamming layout strategy based on the CRB is applicable to a variety of receiving systems.

To obtain a CRB-based optimal model of the layout strategy for distributed jammers, the CRB of the target parameter estimation of UASNs under distributed jammers should be studied. There are studies on the CRB in receiver systems in the presence of multiple targets, mostly under the assumption of a uniform environmental noise field [15–18]. However, the jamming noise received by each node in the sensor network should be nonuniform and related under the influence of distributed jammers, and there is no relevant derivation in the existing literature. Therefore, in this paper, the CRB of UASNs in a nonuniform noise field under a distributed jamming strategy is derived, similar to the derivation used by Stoica and Nehorai [15] under the assumption of a uniform noise background.

According to the obtained CRB, a CRB maximization model with the position of the jammers as a variable is established and used as the basis of the distributed jamming optimization layout strategy. To solve this problem, particle swarm optimization (PSO) is adopted to analyze the distributed jamming strategy proposed in this paper through numerical experiments considering different environmental parameters. The proposed optimal layout strategy can cause higher CRB of the UASN than other traditional layout strategies, which means a stronger jamming effect to the UASN and stronger protection to targets.

The remainder of the paper is organized as follows. The system model of UASNs in the presence of multiple jamming sources is reviewed in Section 2. The CRB of UASNs for multiple target angle estimation in a jamming environment is derived in Section 3. The optimization model of the arrangement of distributed jammers is constructed in Section 4, and numerical results on the performance of the proposed jamming strategy are shown in Section 5. Conclusions are drawn in Section 6.

## 2. System Model

Before this section, some notational conventions used in this paper are shown in Table 1.

**Table 1.** Notations in this paper.

Notation	Description
$E[\cdot]$	the expectation operator; for deterministic signals, $E[\cdot] = \lim_{N \rightarrow \infty} (1/N) \sum_{t=1}^N (\cdot)$
$x^H$	the conjugate transpose of $x$
$x^t$	the transpose of $x$
$\mathbf{A}$	the matrix
$\delta_{m,n}$	the Dirac delta (=1 if $m = n$ and 0 otherwise)

The jamming model studied in this paper consists of three parts: targets, jammers, and the UASN. Assuming they are in a two-dimensional plane, the geometric positions of the targets, jammers, and the UASN are shown in Figure 1. Underwater detection is usually achieved by sonar sensor array and uniform linear array (ULA) is the most common receiver. In this paper, the UASN is a sonar receiving system composed of multiple ULAs, which is also called a networking sonar system and widely used in underwater detection. Suppose the UASN contains  $L$  sensor arrays. Denote the center position of the  $l$ th receiving array as  $(x_{Rl}, y_{Rl})$ , the numbers of elements in the  $l$ th array as  $P_l$ , the space of each element in the  $l$ th array as  $\Delta_l$ , and the tilt angle of the  $l$ th array relative to the  $x$ -axis as  $\gamma_l$ , where  $l = 1, 2, \dots, L$ . Suppose there are  $M$  targets and  $K$  jammers. The position of the  $m$ th target is  $(x_{Tm}, y_{Tm})$ , and the position of the  $k$ th jammer is  $(x_{Jk}, y_{Jk})$ , where  $m = 1, 2, \dots, M$  and  $k = 1, 2, \dots, K$ . The distances between the  $m$ th target and the  $k$ th jammer to the  $l$ th array are

$$d_{Rl}^{Tm} = \sqrt{(x_{Rl} - x_{Tm})^2 + (y_{Rl} - y_{Tm})^2} \tag{1}$$

$$d_{Rl}^{Jk} = \sqrt{(x_{Rl} - x_{Jk})^2 + (y_{Rl} - y_{Jk})^2} \tag{2}$$

The angle between the  $m$ th target and the  $l$ th array (relative to the array normal direction) is

$$\varphi_l^m = \arctan\left(\frac{x_{Rl} - x_{Tm}}{y_{Rl} - y_{Tm}}\right) + \gamma_l \tag{3}$$

Assume that the sensor arrays in Figure 1 are passive arrays and only receive radiation signals from the target and jammers and that there are a variety of environmental noise sources in the environment. Denote the radiation signals from the  $m$ th target as  $s_m(t)$ , the radiation signals from the  $k$ th jammer

as  $n_k(t)$ , and the environmental noise influencing the elements of the  $l$ th array as  $e_l(t)$ . The jamming strategy involved in this paper is barrage jamming; that is, the target signal is covered by high-power noise. The research in this paper is based on the following assumptions:

Firstly: The jamming noise emitted by the interference source  $n_k(t)$  is Gaussian white noise with an average value of 0 and a variance of  $\sigma_k$ . Each jammer transmits signals independently, which means that  $E n_k(t) = 0$ ,  $E n_k(t) n_k^H = \sigma_k I$ , and  $E n_{k_1}(t) n_{k_2}^H = 0$ . Assume that each element in the same array receives the same jamming power.

Secondly: All of the elements receive the same environmental noise power and are independent of each other. The environmental noise on the  $l$ th array  $e_l(t)$  is Gaussian white noise with an average value of 0 and a variance of  $\sigma_0$ , where  $l = 1, 2, \dots, L$ ,  $E e_l(t) = 0$ , and  $E e_l(t) e_l^H(t) = \sigma_0 I$ .

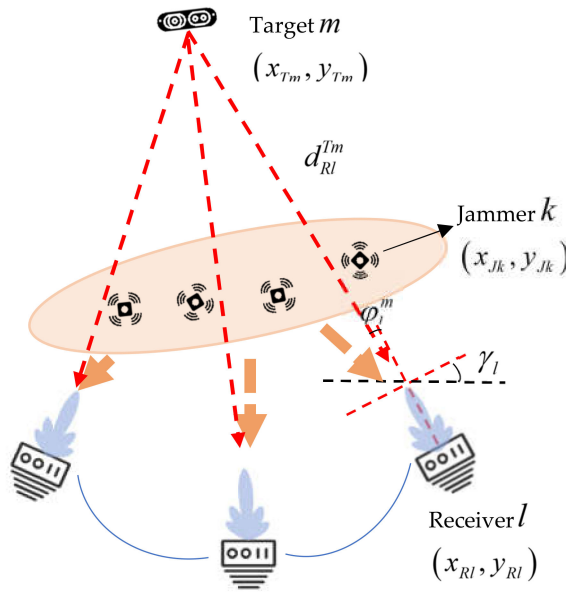


Figure 1. Model of the target, jammer, and sensor network.

Then the received signal model of the  $l$ th array can be expressed as

$$\mathbf{y}_l(t) = \mathbf{A}_l(\boldsymbol{\theta}_T) \hat{\mathbf{s}}(t) + \mathbf{B}_l \hat{\mathbf{n}}(t) + e_l(t) \tag{4}$$

In Equation (4),  $t = 1, 2, \dots, N$ .  $\mathbf{y}_l(t) \in C^{P_l \times 1}$  is the noisy data vector.  $\hat{\mathbf{s}}(t) \in C^{M \times 1}$  is the vector of the target radiation signal amplitudes, and  $\hat{\mathbf{s}}(t) = [s_1(t), \dots, s_m(t)]^t$ .  $\hat{\mathbf{n}}(t) \in C^{K \times 1}$  is the jamming noise, and  $\hat{\mathbf{n}}(t) = [n_1(t), \dots, n_K(t)]^t$ . The matrix  $\mathbf{A}_l(\boldsymbol{\theta}_T) \in C^{P_l \times M}$  has the following structure:

$$\mathbf{A}_l(\boldsymbol{\theta}_T) = \left[ \sqrt{\alpha_{Rl}^{T1}} \mathbf{a}_l(\theta_{T1}), \dots, \sqrt{\alpha_{Rl}^{Tm}} \mathbf{a}_l(\theta_{Tm}) \right] \tag{5}$$

where  $\alpha_{Rl}^{Tm}$  is the propagation loss coefficient from the  $m$ th target to the  $l$ th array and is related to  $d_{Rl}^{Tm}$ .  $\mathbf{a}_l(\theta_{Tm}) \in C^{P_l \times 1}$  is the direction vector from the  $m$ th target to the  $l$ th array. Under the assumption of a uniform linear array (ULA),

$$\mathbf{a}_l(\theta_{Tm}) = \left[ 1, e^{j \frac{2\pi \Delta_l}{\lambda} \sin \theta_{Tm}}, \dots, e^{j (P_l - 1) \frac{2\pi \Delta_l}{\lambda} \sin \theta_{Tm}} \right]^t \tag{6}$$

Under the first assumption, the matrix  $\mathbf{B}_l \in C^{1 \times K}$  can be expressed as

$$\mathbf{B}_l = \left[ \sqrt{\alpha_{Rl}^{J1}} e^{j \frac{2\pi d_{Rl}^{J1}}{\lambda} \sin \theta_{J1}}, \dots, \sqrt{\alpha_{Rl}^{JK}} e^{j \frac{2\pi d_{Rl}^{JK}}{\lambda} \sin \theta_{JK}} \right] \tag{7}$$

where  $\alpha_{RI}^{Jk}$  is the propagation loss from the  $k$ th jammer to the  $l$ th array, which is related to  $d_{RI}^{Jk}$ . In the case of a fixed receiver position  $(x_{RI}, y_{RI})$ ,  $\alpha_{RI}^{Jk}$  depends on the position of the jammer  $(x_{Jk}, y_{Jk})$ .

Since the jamming noise and environmental noise received by the  $l$ th array are both Gaussian white noise and independent from each other, the superimposed noise is still Gaussian white noise, and the total power is the sum of the power of each noise source, which can be expressed as

$$\hat{\sigma}_l = \sum_{k=1}^K \alpha_{RI}^{Jk} \sigma_k + \sigma_0 \tag{8}$$

where  $\sigma_k$  is the noise power emitted by the  $k$ th jammer and  $\alpha_{RI}^{Jk} \sigma_k$  is the noise power of the  $k$ th jammer received by the  $l$ th array.

Thus far, a receiving signal model of an UASN has been provided, which contains multiple targets and barrage jammers. The working principle of the barrage jamming method is to transmit high-power noise and reduce the signal-to-noise ratio of the UASN, thereby increasing its parameter estimation error. Therefore, the jamming effect depends on the noise power. According to Equations (2) and (8), the total power of the array receiving noise is closely related to the locations of the distributed jammers, especially in a sensor network containing multiple arrays. Therefore, the purpose of this paper is to study the optimal layout strategy for suppressing jammers of UASNs. In the next section, the CRB for the joint estimation of UASNs is presented to evaluate the jamming effect of distributed jammers.

### 3. Calculation of the CRB

The CRB is the best accuracy that a receiving system can achieve when estimating the target parameters. The CRB is usually used to measure the receiver performance and is used as a measure of the distributed jamming performance in this paper. In the case of constant target parameters, the higher the CRB of the receiver, the better the jamming effect. In this section, the CRB of the receiving sensor network for target angle estimation is derived, which considers the position of the jammers  $(x_{Jk}, y_{Jk})$  as a variable. Based on this approach, the optimal layout strategy for the distributed jammers based on CRB maximization is presented in the next section. The CRB of a single sensor array with a Gaussian white noise background was given by Stoica and Nehorai [15]; however, this approach cannot be adopted directly in the model of this paper, which contains a 10-array network, where the receiving noise of each array is different but coherent [19] (the noise power of each jammer is superposed).

The CRB of the receiving system can be written as

$$\mathbf{CRB} = \left\{ \mathbb{E} \left[ \frac{\partial^2 \ln L(y|\rho)}{\partial \rho^2} \right] \right\}^{-1} \tag{9}$$

where  $\rho$  is a collection of unknown parameters and  $L(y|\rho)$  is the probability density function of  $\rho$ . In the model described above, the unknown estimated parameters of the receiving system are

$$\rho = \{\hat{\sigma}, \mathcal{R}(\hat{\mathbf{s}}(t)), \mathcal{I}(\hat{\mathbf{s}}(t)), \theta_{\mathbf{T}}\} \tag{10}$$

where  $\hat{\sigma}$  is the array receiving noise and is related to the position of the jammers  $(x_{Jk}, y_{Jk})$ , the emission noise power of the jammers  $\sigma_k$ , and the environmental noise power  $\sigma_0$ ;  $\theta_{\mathbf{T}}$  is the arrival angle of the target signal,  $\mathcal{R}(\hat{\mathbf{s}}(t)) \triangleq \text{Re}\hat{\mathbf{s}}(t)$  is the real part of the target signal, and  $\mathcal{I}(\hat{\mathbf{s}}(t)) \triangleq \text{Im}\hat{\mathbf{s}}(t)$  is the imaginary part of the target signal.

The probability density function of joint estimation of multiple arrays can be written as

$$L(y|\rho) = \frac{1}{\pi^{MN} \det(\mathbf{Q})^{MN}} \exp \left\{ - \sum_{t=1}^N [\tilde{\mathbf{y}}(t) - \tilde{\mathbf{A}}\hat{\mathbf{s}}(t)]^H \mathbf{Q}^{-1} [\tilde{\mathbf{y}}(t) - \tilde{\mathbf{A}}\hat{\mathbf{s}}(t)] \right\} \tag{11}$$

where

$$\mathbf{Q} = \begin{bmatrix} \hat{\sigma}_1 & & \\ & \ddots & \\ & & \hat{\sigma}_L \end{bmatrix} \tag{12}$$

$$\tilde{\mathbf{y}}(t) = [\mathbf{y}_1(t), \dots, \mathbf{y}_L(t)]^t \tag{13}$$

$$\tilde{\mathbf{A}} = [\mathbf{A}_1(\boldsymbol{\theta}_T), \dots, \mathbf{A}_L(\boldsymbol{\theta}_T)]^t \tag{14}$$

$$\mathbf{D}_1 = \frac{\partial \mathbf{A}_1(\boldsymbol{\theta}_T)}{\partial \boldsymbol{\theta}_T} \tag{15}$$

Then according to the derivation method used by Stoica and Nehorai [15], the CRB of the sensor network's estimation of the target angle can be obtained (see the detailed derivation process in Appendix A):

$$\text{CRB}(\boldsymbol{\theta}_T) = \left\{ \boldsymbol{\Gamma} - \sum_{t=1}^N \text{Re}[\mathbf{v}_t^H \mathbf{G} \mathbf{v}_t] \right\}^{-1} \tag{16}$$

where

$$\boldsymbol{\Gamma} = \sum_{i=1}^L \sum_{j=1}^L \frac{2}{\hat{\sigma}_i \hat{\sigma}_j} \left( \sum_{k=1}^K \alpha_{R_i}^{Jk} \alpha_{R_j}^{Jk} \sigma_k \right) \sum_{t=1}^N \text{Re}[\hat{\mathbf{s}}^H(t) \mathbf{D}_i^H \mathbf{D}_j \hat{\mathbf{s}}(t)] \tag{17}$$

$$\mathbf{v}_t = \sum_{i=1}^L \sum_{j=1}^L \frac{2}{\hat{\sigma}_i \hat{\sigma}_j} \left( \sum_{k=1}^K \alpha_{R_i}^{Jk} \alpha_{R_j}^{Jk} \sigma_k \right) \text{Re}[\mathbf{A}_i^H \mathbf{D}_j \hat{\mathbf{s}}(t)] \tag{18}$$

$$\mathbf{G} = \mathbf{H}^{-1} \tag{19}$$

$$\mathbf{H} = \sum_{i=1}^L \sum_{j=1}^L \frac{2}{\hat{\sigma}_i \hat{\sigma}_j} \left( \sum_{k=1}^K \alpha_{R_i}^{Jk} \alpha_{R_j}^{Jk} \sigma_k \right) \mathbf{A}_i^H \mathbf{A}_j \tag{20}$$

The CRB of the target angle estimation in Equation (15) is a function of all parameters of the target, receivers, jammers, and the environment. In this paper, the optimal layout strategy of the jammers is considered, thus the parameters of the target, receiver, and environment can be assumed to be fixed. Under this assumption, the CRB in Equation (15) varies only with the noise power emitted by each jammer  $\sigma_k$  and their locations  $(x_{Jk}, y_{Jk})$ . In practical situations, the available jammer resources are usually known; that is, the jammer transmit power is known. Under this condition, the CRB obtained in this paper is only related to the locations of the jammers. Therefore, by optimizing  $(x_{Jk}, y_{Jk})$ , the maximum CRB can be obtained, thereby obtaining the strongest jamming effect, which can reduce the estimation accuracy of the UASN.

## 4. Distributed Jamming Strategy Design

### 4.1. Optimization Model

According to the CRB obtained in the previous section, a distributed barrage jamming layout strategy for an UASN is proposed, which uses the CRB of the UASN as the evaluation index of jamming effect to find the optimal distribution of jammers, as shown in Figure 2. In this section, the distributed barrage jamming layout strategy is transformed into a mathematical model based on CRB maximization, where the locations of the jammers are used as a variable and the jamming performance is reflected by the jamming noise power.

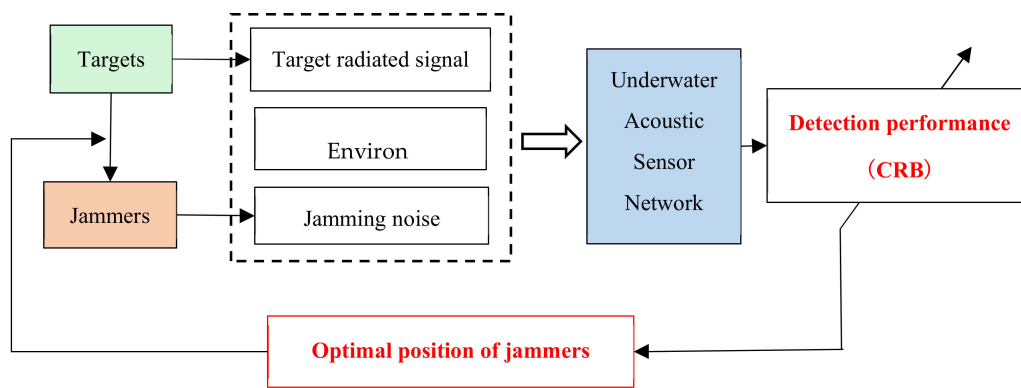


Figure 2. Model of optimal jamming layout strategy. CRB: CraméRao bound.

In the jamming scenario studied in this paper, a self-defense jamming strategy is considered, where the target signals are received by the receiver and the barrage jamming noise is transmitted to the receiver. Thus, the signal-to-noise ratio of the receiver is reduced, and the estimation error of the target is increased, which helps the target escape from the tracking of the UASN. Therefore, the signal of the receiver should include the target radiated signal, the emission noise of each jammer, and the environmental noise, as shown in Equation (4). A low-cost jammer is considered, which can radiate uniform jamming noise in all directions in space, so there is no need to use an array structure to modulate its phase. The use of such jammers can reduce the cost of the entire distributed jamming system, so more jammers can be employed to achieve better effects with complex sensor networks.

Since the jammers are launched by the target, the available jamming resources should be known when the jamming strategy is designed; that is, the number of jammers  $K$ , the emission jamming noise power  $\sigma_k$ , and the location of the jammers  $(x_{Jk}, y_{Jk})$  are known. Suppose that the jammer has obtained some basic information about the receiver through the detection equipment of the target, (e.g., the numbers of arrays  $L$  and the locations of the arrays  $(x_{Rl}, y_{Rl})$ ), then the CRB of the UASN can be obtained.

Under the assumptions in Section 2, the calculation of the total power of the received noise of each array is shown in Equation (8). The total received noise power of each array is the sum of the jamming noise power after propagation attenuation  $\alpha_{Rl}^{Jk}\sigma_k$  and the environmental noise power  $\sigma_0$ . Since distributed jammers are usually distributed near the receivers, the propagation attenuation model of the jamming noise is considered as a spherical attenuation model in this paper. That is

$$\alpha_{Rl}^{Jk} = \frac{1}{(d_{Rl}^{Jk})^2} = \frac{1}{(x_{Rl} - x_{Jk})^2 + (y_{Rl} - y_{Jk})^2} \tag{21}$$

Nevertheless, the propagation attenuation model of jamming noise depends on the actual marine environment and the jammer and receivers. Therefore, other propagation attenuation models can be used according to the actual situation when designing a distributed jamming layout strategy.

In Equation (21),  $\alpha_{Rl}^{Jk}$  depends on the distance between the jammers and the receiver  $d_{Rl}^{Jk}$ . When the receiver distance is known, the total power of the receiver noise is only related to the locations of the jammers  $(x_{Jk}, y_{Jk})$ . In polar coordinates, the locations can be expressed as  $(r_k \sin \theta_{Jk}, r_k \cos \theta_{Jk})$ , where  $r_k$  is the distance from the  $k$ th jammer to the origin of the coordinates. Suppose the  $k$ th jammer is sent by the  $m$ th target; the geometry is shown in Figure 3. Usually, the distance between jammers and the target  $d_{Tm}^{Jk}$  is known; it is the distance travelled by the jammer from the target and always equal to the longest distance that the jammer can travel (to be closer to the receiver to get the maximum jamming

performance). So  $d_{Tm}^{Jk}$  and  $r_k$  can be different for different jammers, and the latter can be calculated from the geometry in Equation (22):

$$\sqrt{(r_k \sin \theta_{Jk} - x_{Tm})^2 + (r_k \cos \theta_{Jk} - y_{Tm})^2} = d_{Tm}^{Jk} \tag{22}$$

Since  $r_k$  can be calculated from the known parameters, the angle of the jammer is the only variable in CRB (Equation (16)). Therefore, the optimal location layout strategy for the distributed jammers can be expressed as the optimal angle layout strategy, which depends on  $\theta_{Jk}$ .

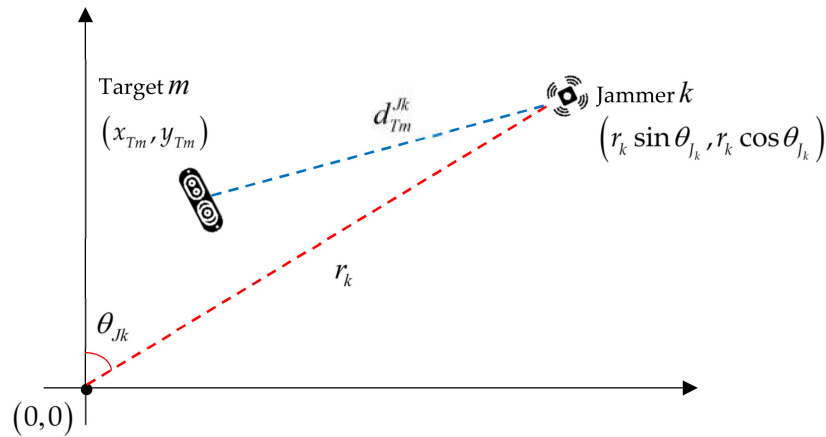


Figure 3. Geometry of the  $m$ th target and the  $k$ th jammer.

After clarifying the parameters of each component in the jamming scenario, an optimization model of the distributed jammer layout strategy based on CRB maximization is designed. The CRB of the UASN for the target angle estimation is given in Equation (16). For  $M$  targets, the resulting CRB is an  $M \times M$  matrix, and the diagonal elements of the matrix are the estimated variances of the angles of each target.

$$\begin{cases} C_{\theta_{T1}} = [\mathbf{CRB}_{\theta_T}]_{1,1} \\ C_{\theta_{T2}} = [\mathbf{CRB}_{\theta_T}]_{2,2} \\ \dots \\ C_{\theta_{Tm}} = [\mathbf{CRB}_{\theta_T}]_{M,M} \end{cases} \tag{23}$$

By maximizing the weighted average CRB for the estimation of each target angle, the optimal angle of the jammers can be obtained

$$\begin{aligned} & \max_{\theta_{J1}, \dots, \theta_{J2}} \sum_{m=1}^M \lambda_m C_m \\ & \text{s.t. } \hat{\sigma}_l = \sum_{k=1}^K \alpha_{Rl}^{Jk} \sigma_k + \sigma_0 \\ & \alpha_{Rl}^{Jk} = \frac{1}{(x_{Rl} - x_{Jk})^2 + (y_{Rl} - y_{Jk})^2} \\ & (x_{Jk}, y_{Jk}) = (r_k \sin \theta_{Jk}, r_k \cos \theta_{Jk}) \end{aligned} \tag{24}$$

where  $\lambda_1, \dots, \lambda_M$  are regularization factors that can be determined according to the importance of the corresponding target.

#### 4.2. Problem Solution

The optimal layout strategy model for distributed jammers provided in this paper is based on a calculation of the CRB. Since the calculation formula of the CRB is very complicated, integrating

various parameters of the receiving system and the received system, and highly nonconvex, heuristic algorithms can be used. Common heuristic algorithms include simulated annealing, greedy algorithms, tabu search, ant colony optimization, and genetic algorithms [20–25]. This paper uses particle swarm optimization (PSO) [24,25] to solve the given optimization problem. PSO is an iterative global optimization algorithm with simple parameters and an easy implementation, which is widely used in various complex nonconvex function optimization problems.

PSO is an evolutionary computing technology that was proposed by Eberhart and Kennedy in 1995 [25]. PSO simulates the flight and foraging behavior of bird swarms; it is a simplified model based on swarm intelligence. Each optimization problem solution is imagined as a bird, called a particle. All particles are searched in a given  $D$ -dimensional space, and the search fitness value is calculated by a given fitness function to judge the current search position  $\mathbf{x}_i^{(n)}$ , where  $\mathbf{x}_i^{(n)} = [x_{i1}^{(n)}, \dots, x_{iD}^{(n)}]$ . Each particle records the best position  $\mathbf{pbest}_i^{(n)}$  searched so far and uses a speed  $\mathbf{v}_i^{(n)}$  to determine the direction and step size of the next iteration, where  $\mathbf{pbest}_i^{(n)} = [pbest_{i1}^{(n)}, \dots, pbest_{iD}^{(n)}]$  and  $\mathbf{v}_i^{(n)} = [v_{i1}^{(n)}, \dots, v_{iD}^{(n)}]$ . The fitness values of all particles are compared to obtain the best position acquired by the population  $\mathbf{gbest}^{(n)}$ , where  $\mathbf{gbest}^{(n)} = [gbest_1^{(n)}, \dots, gbest_d^{(n)}]$ . The iteration formulas of the speed in each dimension  $v_{id}^{(n)}$  and the position in each dimension  $x_{id}^{(n)}$  in the PSO algorithm are

$$\begin{aligned} v_{id}^{(n)} &= wv_{id}^{(n-1)} + c_1r_1(pbest_{id} - x_{id}^{(n-1)}) + c_2r_2(gbest_d^{(n-1)} - x_{id}^{(n-1)}) \\ x_{id}^{(n)} &= x_{id}^{(n-1)} + v_{id}^{(n-1)} \end{aligned} \tag{25}$$

where  $c_1$  and  $c_2$  are the acceleration constants,  $r_1$  and  $r_2$  are random functions, and  $w$  is the inertia weight. The specific parameter settings are described in detail by Kennedy and Eberhart [25] and Poli and colleagues [26].

In the optimization model of this paper, the final solution should be the angles of  $K$  jammers. Therefore, the dimension of each particle should be set as  $D = K$ , and the position of each particle should be set as  $x_{id} = \theta_{J_k}$ . According to the block diagram of the PSO algorithm (Figure 4), the optimal location of each jammer can be obtained.

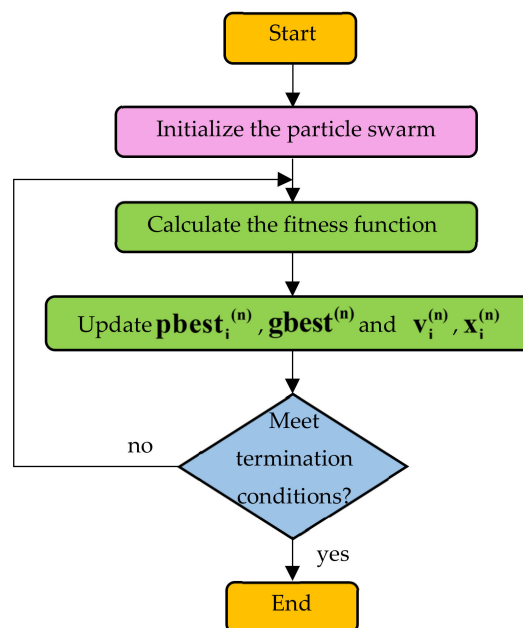


Figure 4. Flow chart of particle swarm optimization (PSO).

### 5. Numerical Experiments

In this section, the effectiveness of the proposed jamming strategy is analyzed through numerical simulation experiments. The jamming scenario in this paper includes an UASN (consisting of three ULAs), targets, distributed jammers, and environmental noise. Therefore, different array parameters, environmental noise, and target parameters are considered to study their impact on the optimal placement angle of the distributed jammers. In addition, different layout strategies are compared, including (1) concentrated (all of the jammers are concentrated using the array angle with better detection performance); (2) random (the jammers are randomly distributed in all array directions); (3) uniform (the jammers are distributed between array angles of arrays at equal intervals); and (4) optimized (the proposed layout strategy in this paper) layouts.

#### 5.1. Influence of the Sensor Networks

First, the influence of the sensor network on the optimal distribution angle should be considered. The array angle, the distance between the array and the target, and the number of array elements in each array are set as variables, because all three parameters will affect the target detection performance of the sensor network. In the simulations in this section, a single target scenario is considered in which the target’s location is set to (0, 0), and the target radiated signal is assumed to be Gaussian white noise with a power of 110 dB. Meanwhile, three arrays, whose normal directions point to the target, and the environmental noise received by the array elements, which is Gaussian white noise with a power of 50 dB, compose the sensor network at the same time. The jammer, which is 2000 m away from the target, emits Gaussian white noise with a power of 110 dB. The tables below show the results of the following three simulations under different scenarios:

- (1) The distribution angle (relative to the target) of each array is used as a variable. The distance of each array to the target is 2500 m, and all the arrays are eight-element ULAs;
- (2) The distance of each array to the target is used as a variable. The angles of the arrays are 10°, 30°, and 50°, and all the arrays are eight-element ULAs;
- (3) The element numbers of each array are used as a variable. The distance of each array to the target is 2500 m, the angles of the arrays are 10°, 30°, and 50°, and all the arrays are eight-element ULAs.

The first simulation of this section assumes that each array in the sensor network has the same array structure and the same distance to the target, which means that every array has the same target detection performance. From the calculation results of the three jammers in Table 2, it can be seen that when the detection performance of each array is the same, the jammers tend to be placed between each array and the target. The calculation results of the six jammers indicate the same conclusion. When the jammers cannot be evenly distributed among the array element angles (the number of jammers cannot be divided by the number of arrays), such as the case of four jammers, it can be found that three of the jammers are still distributed on the lines between each array and the target. The other jammer can be placed on any of the array elements randomly.

**Table 2.** Optimized angles of the jammers for different numbers of jammers with respect to the three-array networks with different angles in a single-target scene.

Angles of the Arrays (in °)	Angles of the Jammers (in °)		
	3 jammers	4 jammers	6 jammers
3 arrays			
(10, 30, 50)	(11.8, 29.9, 48.4)	(11.0, 29.8, 30.1, 48.7)	(11.8, 12.3, 29.8, 29.9, 47.8, 48.4)
(10, 40, 70)	(10.6, 40.0, 69.0)	(10.5, 40.0, 40.1, 69.4)	(10.9, 11.3, 39.8, 39.9, 68.9, 69.2)
(0, 20, 60)	(2.1, 18.2, 59.6)	(1.9, 17.5, 58.6, 59.3)	(2.0, 2.3, 17.9, 18.2, 59.5, 59.7)
(0, 20, 80)	(2.5, 17.9, 80.0)	(1.8, 17.7, 79.5, 79.7)	(2.0, 2.1, 17.9, 18.8, 79.9, 80.4)

The second simulation of this section assumes that each array in the UASN has the same array structure and fixed angles, so the closer the array is to the target, the better the detection performance.

From the calculation results of the three jammers in Table 3, it can be seen that when the differences among the distances of the arrays are small, the jammers still tend to be distributed in the same way as the array angles. However, there also exists a tendency for the jammers to gather at arrays that have stronger detection performance. The tendency is more pronounced when the differences among the distances of the arrays are larger. When the difference reaches a certain level, all of the jammers will focus on the array with the strongest detection performance, which means that the jamming system is equivalent to a centralized jamming system. The case with four jammers produces similar results, and when the detection performance of each array is different, the remaining jammers after the equalization will focus on the array angle with the strongest detection performance.

**Table 3.** Optimized angles of the jammers for different numbers of jammers with respect to the three-array networks with different distances in a single-target scene.

Angles of the Arrays (in °)	Distances of Arrays (in m)	Angles of the Jammers (in °)	
		3 jammers	4 jammers
(10, 30, 50)	3 arrays		
	(2600, 2500, 2600)	(13.1, 30.0, 46.8)	(11.9, 29.9, 30.4, 47.8)
	(2700, 2500, 2700)	(15.8, 29.7, 44.5)	(13.4, 30.1, 30.1, 46.7)
	(2700, 2500, 2900)	(15.1, 31.7, 31.9)	(13.6, 31.2, 31.5, 31.7)
	(2900, 2500, 2900)	(29.8, 30.0, 30.1)	(29.6, 30.0, 30.0, 30.2)

The third simulation of this section assumes that the distance from each array to the target in the UASN is equal and the angles are fixed. The more elements the array contains, the better the detection performance. The results in Table 4 are similar to those in Table 3. As the difference in the array detection performance increases, the angles of the jammers tend to be distributed evenly across the arrays and tend to be concentrated at arrays with the highest performance.

**Table 4.** Optimized angles of the jammers for different numbers of jammers with respect to the three-array networks with different numbers of elements in a single-target scene.

Angles of the Arrays (in °)	Numbers of Elements	Angles of the Jammers (in °)	
		3 jammers	4 jammers
(10, 30, 50)	3 arrays		
	(8, 10, 8)	(14.2, 30.2, 46.1)	(12.3, 29.7, 30.0, 48.1)
	(8, 11, 8)	(16.4, 30.1, 43.4)	(13.3, 29.9, 30.3, 46.9)
	(8, 11, 10)	(27.3, 27.5, 48.1)	(13.3, 31.1, 31.4, 48.5)
	(8, 12, 8)	(30.0, 30.0, 30.1)	(27.0, 27.3, 27.4, 46.0)

### 5.2. Influence of Environmental Noise

This section considers the influence of environmental noise on the optimal angles of distributed jammers, and the simulation scenario is the same as in Section 5.1. The UASN consists of three 8-element ULAs, and the angles of the array relative to the target are fixed to (10°, 30°, 50°). Assuming that the distance from each array to the target is fixed at (2600 m, 2500 m, 2600 m), in this sensor network, the array at 30° has the strongest detection performance. In the second case, the distance from each array to the target is fixed to (2500 m, 2500 m, 2500 m), and then the receiving performance of each array in this sensor network is the same. Table 5 shows the results of the optimal jamming angles under environmental noise with different values of the variance  $\sigma_0$ . Another case adopts the centralized layout strategy, random layout strategy, uniform layout strategy, and optimal layout strategy under environmental noise with different variances. The results of the second case are all indicated in Figure 5.

**Table 5.** Optimized angles of three jammers with respect to the three-array networks under environmental noise with different variances in a single-target scene.

Environmental Noise Variance $\sigma_0$ (in dB)	Angles of the Jammers in the First Situation (in $^\circ$ )	Angles of the Jammers in the Second Situation (in $^\circ$ )
40	(12.9, 29.8, 47.3)	(11.1, 30.0, 48.1)
50	(13.2, 29.9, 46.9)	(11.8, 30.2, 48.2)
60	(29.9, 30.1, 30.2)	(12.4, 30.3, 47.8)
70	(29.9, 30.0, 30.2)	(30.1, 30.1, 30.2)

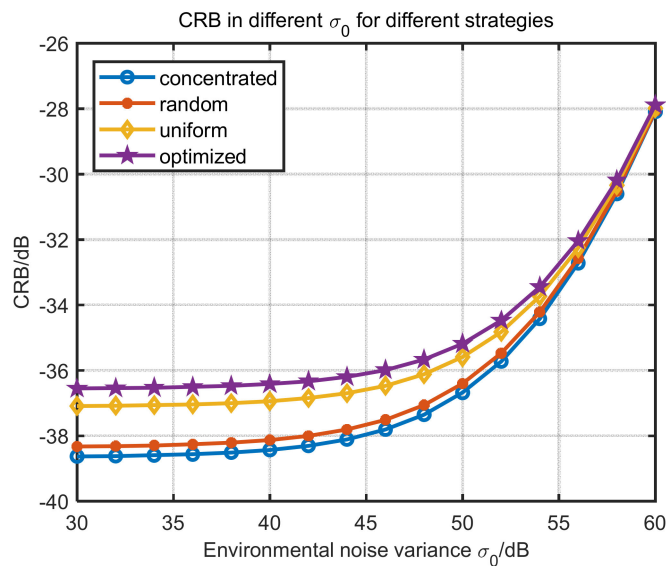


**Figure 5.** Cramér–Rao bound (CRB) under environmental noise with different variances for different strategies in a single-target scene.

In the first case, the simulation assumes that the array with the  $30^\circ$  direction is closest to the target, so it has the strongest detection performance. Table 5 shows that when the variance of the environmental noise is small, the optimal angles of the jammers are consistent with the conclusion in Section 5.1 (i.e., they are close to the array angles, and when the variance of the environmental noise gradually increases, the optimal angles of the jammers tend to become compact). The second case shows that regardless of whether the array detection performance is the same, the optimal angle of each jammer is concentrated in the array in the middle of the sensor network as long as the environmental variance is large enough.

Figure 5 indicates that the proposed optimization strategy has a higher CRB of the target angle estimation than the other three strategies, especially in the case of low environmental noise. The CRBs obtained by the four strategies are not very different under high environmental noise, because the noise signal affecting the receiver in this case is mainly environmental noise. Therefore, the proposed optimal distributed jamming layout strategy has greater advantages in the case of low environmental noise.

### 5.3. Multitarget Scene

In this section, the optimal layout strategy for distributed jammers in a multitarget scenario is considered, which contains three targets with the same power as the radiation signal and are located at (0,0), (2000,0), and (0,1000) (the unit is m). Assuming that every target is equally important, the regularization factor in Equation (23) is  $\lambda_1 = \lambda_2 = \lambda_3 = 1/3$ . Similarly, three eight-element ULAs are used. The angle of each array with respect to the target is fixed at  $(10^\circ, 30^\circ, 50^\circ)$ , and the distance from each array to the target is fixed at (2500 m, 2500 m, 2500 m). Six jammers with an emission noise power of 110 dB are used. Based on the jamming scenario in Figure 1, the optimal angles for  $\sigma_0 = 30$  dB

are indicated in Figure 6. Then, in the case of  $\sigma_0 = 30 \sim 60$  dB, four different jamming strategies are adopted, and the CRBs are indicated in Figure 7.

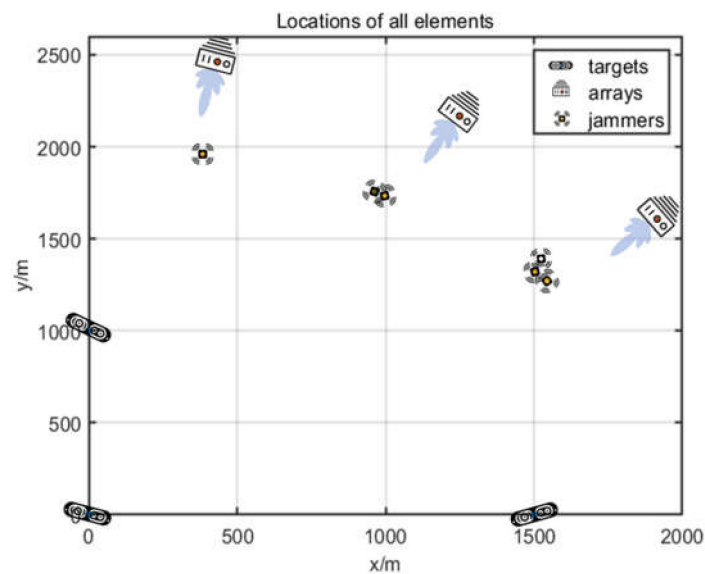


Figure 6. Locations of the elements in the model of a multitarget scene.

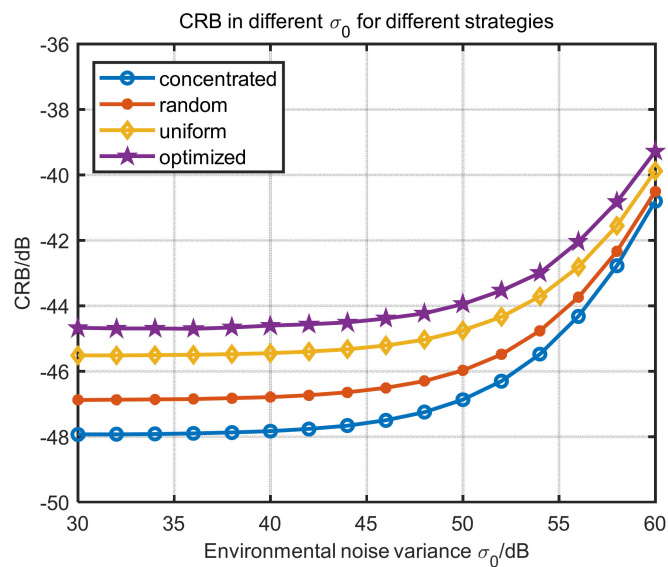
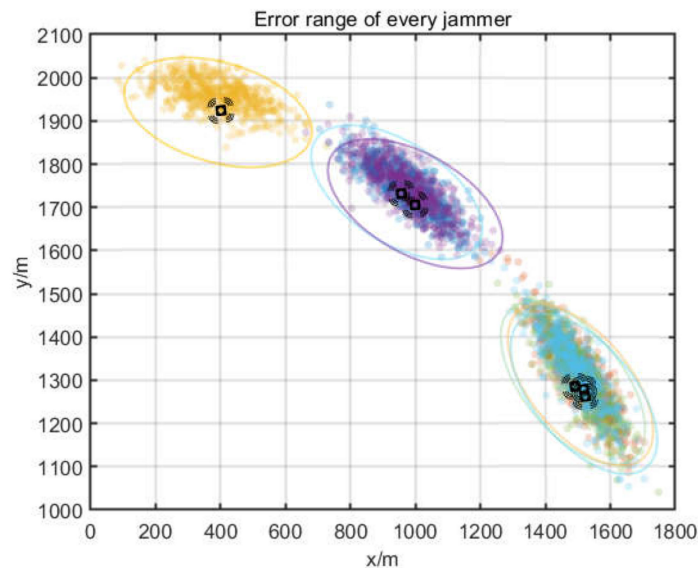


Figure 7. CRB under different environmental noise for different strategies in a multitarget scene.

Figure 6 shows that in the case of multiple targets, the jammers still tend to be distributed according to the array angles. Since distributed jamming is usually a short-range jamming method, the optimal distribution of the angles of the jammers has a greater relationship with the structure of the sensor network. Figure 7 shows the CRB of the target angle estimation of the sensor network obtained by using the concentrated layout strategy, random layout strategy, uniform layout strategy, and optimal layout strategy under different environmental noise conditions; from the results, we find that the proposed strategy has the highest CRB among these strategies, which means it has the strongest impact on the receiver’s parameter estimation performance. That is, the proposed optimal strategy can also achieve better jamming performance than the other strategies in a multitarget scenario.

#### 5.4. Analysis of the Position Error

There is strong turbulence in a real marine environment, which can have a non-negligible effect on the position of an underwater combat platform. Thus, the real position of the jammers will deviate greatly from the original position. In this section, the location error of the jammers is discussed to verify the effectiveness of the proposed optimized layout strategy. The multitarget scenario is considered, and the parameters of the targets and UASN in this section are the same as those in Section 5.3. Assuming that the distance error of the jammer caused by factors such as ocean turbulence and wind follows a normal distribution with a mean of 0 and a standard deviation of 30 m, the angle error of the jammer follows a normal distribution with a mean of 0 and a standard deviation of 3°. Due to the errors, the actual position of the jammer will fluctuate around the calculated value, so the CRB calculated from the actual position will also fluctuate near the theoretical value. Figure 8 shows the possible locations of jammers for  $\sigma_0 = 30$  dB in the presence of errors. The fluctuation range of the CRB obtained by the proposed optimized layout strategy in the presence of location errors is indicated in Figure 9. Since the uniform layout strategy achieves better jamming performance than the random layout strategy and concentrated layout strategy, the uniform layout strategy is used for a comparison with the optimized strategy.



**Figure 8.** Range of the real locations of the jammers.

Figure 8 shows obvious error in the location of the jammers compared with the calculated optimal location, and Figure 9 presents the calculated CRB under this error condition. It is obvious that the proposed optimal layout strategy achieves a better performance than the uniform layout strategy. The lower bound of the CRB fluctuation range caused by the position error of the jammers with the optimized strategy is higher than the upper bound of the CRB fluctuation range with the uniform strategy for most environmental noise conditions. The CRB fluctuation range is roughly the same for both the optimized strategy and the uniform strategy, so it can be inferred that for the random layout strategy and the centralized layout strategy, the CRB fluctuation range is also roughly the same and lower. Thus, the proposed optimal strategy still achieves the best jamming performance when there is a deviation in the real location of the jammers. It can also be found that as the environmental noise increases, the fluctuation in the CRB caused by the position error of the jammers decreases, which means that the real position of the jammers will not affect the jamming effect. This is because the main barrage effect for the UASN comes from environmental noise in this case. From the experiment in this section, a situation close to the real marine environment is considered. The result has proven that the

optimal strategy proposed in this paper still achieves a significantly better jamming performance even in the case of uncertain errors, which verifies its practicability.

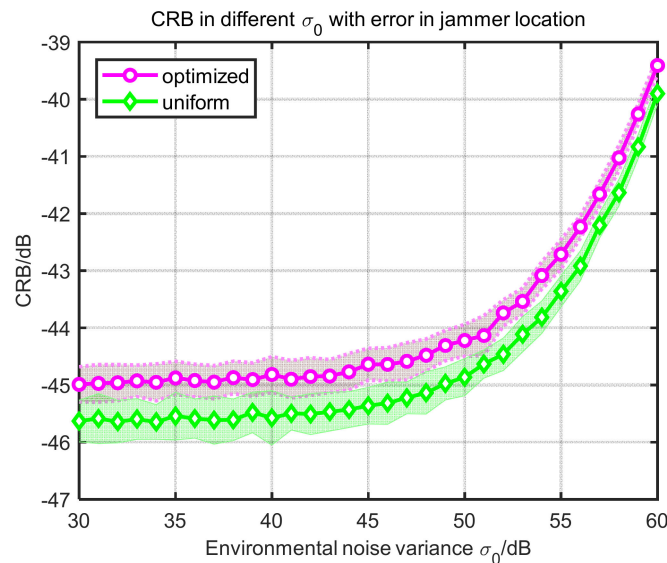


**Figure 9.** CRB under environmental noise with different variances.

## 6. Conclusions

In this paper, the optimal layout strategy for distributed barrage jammers against UASNs is studied. The CRB of UASNs estimating target angles in the case of multiple targets and multiple jammers is derived, which uses the angle of the jammers as a variable. Based on this result, a distributed jamming optimization strategy is proposed, which uses the maximum CRB as the cost function and aims to obtain the optimal distribution of the jammers. PSO algorithm is used to solve this complex and nonconvex model. Numerical experiments are executed to compare the jamming strategy with three traditional strategies. The results show that the proposed optimal layout strategy for distributed jammers can achieve stronger jamming effects than the other strategies. The position error of the jammers caused by turbulence and a hurricane in a real ocean is considered, and the result shows that the proposed optimal layout strategy still performs better than the other strategies under obvious error conditions.

Future research will focus on more efficient jamming strategies to adapt to complex real-world scenarios, including using the mix jamming method of barrage jammers and deceptive jammers and increasing the speed of algorithm operations.

**Author Contributions:** Conceptualization, J.Z. and Y.D.; methodology, M.X. and J.Z.; software, M.X. and X.J.; investigation, Y.D.; writing—original draft preparation, M.X. and X.J.; writing—review and editing, M.X., J.Z., Y.D. and X.J.; supervision, J.Z. and Y.D.; project administration, J.Z.; funding acquisition, M.X. and J.Z. All authors have read and agreed to the published version of the manuscript.

**Funding:** This research was sponsored by the National Key R&D Program of China, No. 2016YFC1400104, and the Seed Foundation of Innovation and Creation for Graduate Students in Northwestern Polytechnical University, No. ZZ2019005.

**Acknowledgments:** We appreciate all editors and reviewers for the valuable suggestions and constructive comments. Thank you to everyone who contributed to this article.

**Conflicts of Interest:** The authors declare no conflicts of interest.

**Appendix A**

As shown in Equation (11), the joint likelihood function of the data received by UASNs is

$$L(y|\rho) = \frac{1}{\pi^{MN} \det(\mathbf{Q})^{MN}} \exp\left\{-\sum_{t=1}^N [\tilde{\mathbf{y}}(t) - \tilde{\mathbf{A}}\hat{\mathbf{s}}(t)]^H \mathbf{Q}^{-1} [\tilde{\mathbf{y}}(t) - \tilde{\mathbf{A}}\hat{\mathbf{s}}(t)]\right\} \tag{A1}$$

Thus, the log-likelihood function is

$$\ln L = \text{const} - mN \ln \prod_{l=1}^L \hat{\sigma}_l - \sum_{t=1}^N \sum_{l=1}^L \frac{1}{\hat{\sigma}_l} [\mathbf{y}_1(t) - \mathbf{A}_l \hat{\mathbf{s}}(t)]^H [\mathbf{y}_1(t) - \mathbf{A}_l \hat{\mathbf{s}}(t)] \tag{A2}$$

Denote  $\mathbf{g}_l(t) = \mathbf{B}_l \hat{\mathbf{n}}(t) + e(t)$ , as the total noise received by the  $l$ th sensor array. The derivatives of Equation (A2) with respect to  $\mathcal{R}(\hat{\mathbf{s}}(t))$ ,  $\mathcal{I}(\hat{\mathbf{s}}(t))$ , and  $\theta_{\mathbf{T}}$  are

$$\frac{\partial \ln L}{\partial \mathcal{R}(\hat{\mathbf{s}}(t))} = \sum_{l=1}^L \frac{2}{\hat{\sigma}_l} \text{Re}[\mathbf{A}_l^H \mathbf{g}_l(t)] \quad t = 1, \dots, N \tag{A3}$$

$$\frac{\partial \ln L}{\partial \mathcal{I}(\hat{\mathbf{s}}(t))} = \sum_{l=1}^L \frac{2}{\hat{\sigma}_l} \text{Im}[\mathbf{A}_l^H \mathbf{g}_l(t)] \quad t = 1, \dots, N \tag{A4}$$

$$\frac{\partial \ln L}{\partial \theta_{\mathbf{T}}} = \sum_{l=1}^L \frac{2}{\hat{\sigma}_l} \sum_{t=1}^N \text{Re}[\hat{\mathbf{s}}^H(t) \mathbf{D}_l^H \mathbf{g}_l(t)] \quad t = 1, \dots, N \tag{A5}$$

with

$$\text{Re}(x)\text{Re}(y^t) = \frac{1}{2} [\text{Re}(xy^t) + \text{Re}(xy^H)]$$

$$\text{Im}(x)\text{Im}(y^t) = -\frac{1}{2} [\text{Re}(xy^t) - \text{Re}(xy^H)]$$

$$\text{Re}(x)\text{Im}(y^t) = \frac{1}{2} [\text{Im}(xy^t) - \text{Im}(xy^H)]$$

we have

$$\mathbb{E} \left[ \frac{\partial \ln L}{\partial \mathcal{R}(\hat{\mathbf{s}}(m))} \right] \left[ \frac{\partial \ln L}{\partial \mathcal{R}(\hat{\mathbf{s}}(n))} \right]^t = \sum_{i=1}^L \sum_{j=1}^L \frac{2}{\hat{\sigma}_i \hat{\sigma}_j} \left( \sum_{k=1}^K \alpha_{R_i}^{Jk} \alpha_{R_j}^{Jk} \sigma_k \right) \text{Re}[\mathbf{A}_i^H \mathbf{A}_j] \delta_{m,n} \tag{A6}$$

$$\mathbb{E} \left[ \frac{\partial \ln L}{\partial \mathcal{R}(\hat{\mathbf{s}}(m))} \right] \left[ \frac{\partial \ln L}{\partial \mathcal{I}(\hat{\mathbf{s}}(n))} \right]^t = -\sum_{i=1}^L \sum_{j=1}^L \frac{2}{\hat{\sigma}_i \hat{\sigma}_j} \left( \sum_{k=1}^K \alpha_{R_i}^{Jk} \alpha_{R_j}^{Jk} \sigma_k \right) \text{Re}[\mathbf{A}_i^H \mathbf{A}_j] \delta_{m,n} \tag{A7}$$

$$\mathbb{E} \left[ \frac{\partial \ln L}{\partial \mathcal{R}(\hat{\mathbf{s}}(t))} \right] \left[ \frac{\partial \ln L}{\partial \theta_{\mathbf{T}}} \right]^t = \sum_{i=1}^L \sum_{j=1}^L \frac{2}{\hat{\sigma}_i \hat{\sigma}_j} \left( \sum_{k=1}^K \alpha_{R_i}^{Jk} \alpha_{R_j}^{Jk} \sigma_k \right) \text{Re}[\mathbf{A}_i^H \mathbf{D}_j \hat{\mathbf{s}}(t)] \tag{A8}$$

$$\mathbb{E} \left[ \frac{\partial \ln L}{\partial \mathcal{I}(\hat{\mathbf{s}}(m))} \right] \left[ \frac{\partial \ln L}{\partial \mathcal{I}(\hat{\mathbf{s}}(n))} \right]^t = \sum_{i=1}^L \sum_{j=1}^L \frac{2}{\hat{\sigma}_i \hat{\sigma}_j} \left( \sum_{k=1}^K \alpha_{R_i}^{Jk} \alpha_{R_j}^{Jk} \sigma_k \right) \text{Re}[\mathbf{A}_i^H \mathbf{A}_j] \delta_{m,n} \tag{A9}$$

$$\mathbb{E} \left[ \frac{\partial \ln L}{\partial \theta_{\mathbf{T}}} \right] \left[ \frac{\partial \ln L}{\partial \theta_{\mathbf{T}}} \right]^t = \sum_{i=1}^L \sum_{j=1}^L \frac{2}{\hat{\sigma}_i \hat{\sigma}_j} \left( \sum_{k=1}^K \alpha_{R_i}^{Jk} \alpha_{R_j}^{Jk} \sigma_k \right) \sum_{t=1}^N \text{Re}[\hat{\mathbf{s}}(t)^H \mathbf{D}_i^H \mathbf{D}_j \hat{\mathbf{s}}(t)] \tag{A10}$$

where  $m = 1, \dots, N$  and  $n = 1, \dots, N$ .  $\delta_{m,n}$  is the Dirac delta function ( $\delta_{m,n} = 1$  if  $m = n$  and  $\delta_{m,n} = 0$  otherwise).

Introduce the following notations

$$\Gamma = \sum_{i=1}^L \sum_{j=1}^L \frac{2}{\hat{\sigma}_i \hat{\sigma}_j} \left( \sum_{k=1}^K \alpha_{R_i}^{Jk} \alpha_{R_j}^{Jk} \sigma_k \right) \sum_{t=1}^N \text{Re}[\hat{\mathbf{s}}^H(t) \mathbf{D}_i^H \mathbf{D}_j \hat{\mathbf{s}}(t)] \quad (\text{A11})$$

$$\mathbf{V}_t = \sum_{i=1}^L \sum_{j=1}^L \frac{2}{\hat{\sigma}_i \hat{\sigma}_j} \left( \sum_{k=1}^K \alpha_{R_i}^{Jk} \alpha_{R_j}^{Jk} \sigma_k \right) \text{Re}[\mathbf{A}_i^H \mathbf{D}_j \hat{\mathbf{s}}(t)] \quad (\text{A12})$$

$$\mathbf{G} = \mathbf{H}^{-1} \quad (\text{A13})$$

$$\mathbf{H} = \sum_{i=1}^L \sum_{j=1}^L \frac{2}{\hat{\sigma}_i \hat{\sigma}_j} \left( \sum_{k=1}^K \alpha_{R_i}^{Jk} \alpha_{R_j}^{Jk} \sigma_k \right) \mathbf{A}_i^H \mathbf{A}_j \quad (\text{A14})$$

The analysis of the CRB matrix is the same as in the study by Xiao and colleagues [14], so the CRB can be expressed as

$$\text{CRB}(\boldsymbol{\theta}) = \left\{ \Gamma - \sum_{t=1}^N \text{Re}[\mathbf{V}_t^H \mathbf{G} \mathbf{V}_t] \right\}^{-1} \quad (\text{A15})$$

## References

1. Heidemann, J.; Stojanovic, M.; Zorzi, M. Underwater sensor networks: applications, advances and challenges. *Philos. Trans. R. Soc. A Math. Phys. Eng. Sci.* **2012**, *370*, 158–175. [[CrossRef](#)] [[PubMed](#)]
2. Faheem, M.; Butt, R.A.; Raza, B.; Alquhayz, H.; Ashraf, M.W.; Shah, S.B.; Ngadi, M.A.; Gungor, V.C. QoS-RP: A Cross-Layer QoS Channel-Aware Routing Protocol for the Internet of Underwater Acoustic Sensor Networks. *Sensors* **2019**, *19*, 4762. [[CrossRef](#)] [[PubMed](#)]
3. Sendra, S.; Lloret, J.; Jimenez, J.M.; Parra, L. Underwater Acoustic Modems. *IEEE Sens. J.* **2016**, *16*, 4063–4071. [[CrossRef](#)]
4. Chandrasekhar, V.; Seah, W.K.; Choo, Y.S.; Ee, H.V. Localization in underwater sensor networks: Survey and challenges. In Proceedings of the 1st ACM international workshop on Underwater networks, Los Angeles, CA, USA, 21–25 September 2006; pp. 33–40.
5. Misra, S.; Dash, S.; Khatua, M.; Vasilakos, A.V.; Obaidat, M.S. Jamming in underwater sensor networks: detection and mitigation. *IET Commun.* **2012**, *6*, 2178–2188. [[CrossRef](#)]
6. Apek, O.; Tidhar, G.; Goichman, T. Distributed Jammer System. U.S. Patent No. 7,920,255, 5 April 2011.
7. Song, X.; Willett, P.; Zhou, S.; Luh, P.B. The MIMO Radar and Jammer Games. *IEEE Trans. Signal Process.* **2012**, *60*, 687–699. [[CrossRef](#)]
8. Deligiannis, A.; Rossetti, G.; Panoui, A.; Lambotaran, S.; Chambers, J.A. Power allocation game between a radar network and multiple jammers. In Proceedings of the 2016 IEEE Radar Conference (RadarConf), IEEE, Philadelphia, PA, USA, 2–6 May 2016; pp. 1–5.
9. Zheng, G.; Na, S.; Huang, T.; Wang, L. A barrage jamming strategy based on CRB maximization against distributed MIMO radar. *Sensors* **2019**, *19*, 2453. [[CrossRef](#)] [[PubMed](#)]
10. Kashyap, A.; Basar, T.; Srikant, R. Correlated jamming on MIMO Gaussian fading channels. *IEEE Trans. Inf. Theory* **2004**, *50*, 2119–2123. [[CrossRef](#)]
11. Chavali, P.; Nehorai, A. Scheduling and power allocation in a cognitive radar network for multiple-target tracking. *IEEE Trans. Signal Process.* **2011**, *60*, 715–729. [[CrossRef](#)]
12. Akyildiz, I.F.; Pompili, D.; Melodia, T. Underwater acoustic sensor networks: research challenges. *Ad Hoc Netw.* **2005**, *3*, 257–279. [[CrossRef](#)]
13. Vadori, V.; Scalabrin, M.; Guglielmi, A.V.; Badia, L. Jamming in underwater sensor networks as a Bayesian zero-sum game with position uncertainty. In Proceedings of the 2015 IEEE Global Communications Conference (GLOBECOM), IEEE, San Diego, CA, USA, 6–10 December 2015; pp. 1–6.
14. Xiao, L.; Li, Q.; Chen, T.; Cheng, E.; Dai, H. Jamming games in underwater sensor networks with reinforcement learning. In Proceedings of the 2015 IEEE Global Communications Conference (GLOBECOM), IEEE, San Diego, CA, USA, 6–10 December 2015; pp. 1–6.

15. Stoica, P.; Nehorai, A. MUSIC, maximum likelihood, and Cramer-Rao bound. *IEEE Trans. Acoust. Speech Signal Process.* **1989**, *37*, 720–741. [[CrossRef](#)]
16. Yip, L.; Chen, J.C.; Hudson, R.E.; Yao, K. Cramer-Rao bound analysis of wideband source localization and DOA estimation. In Proceedings of the Advanced Signal Processing Algorithms, Architectures, and Implementations XII, International Society for Optics and Photonics, Seattle, WA, USA, 6 December 2002; Volume 4791, pp. 304–316.
17. Vu, P.; Haimovich, A.M.; Himed, B. Bayesian Cramer-Rao Bound for multiple targets tracking in MIMO radar. In Proceedings of the 2017 IEEE Radar Conference (RadarConf), IEEE, Seattle, WA, USA, 8–12 May 2017; pp. 938–942.
18. Chen, J.C.; Hudson, R.E.; Yao, K. Maximum-likelihood source localization and unknown sensor location estimation for wideband signals in the near-field. *IEEE Trans. Signal Process.* **2002**, *50*, 1843–1854. [[CrossRef](#)]
19. Lu, L.; Wu, H.C.; Yan, K.; Iyengar, S.S. Robust expectation-maximization algorithm for multiple wideband acoustic source localization in the presence of nonuniform noise variances. *IEEE Sens. J.* **2010**, *11*, 536–544. [[CrossRef](#)]
20. Siddique, N.; Adeli, H. Simulated annealing, its variants and engineering applications. *Int. J. Artif. Intell. Tools* **2016**, *25*, 1630001. [[CrossRef](#)]
21. Wang, Y.; Cong, G.; Song, G.; Xie, K. Community-based greedy algorithm for mining top-k influential nodes in mobile social networks. In Proceedings of the 16th ACM SIGKDD international conference on Knowledge discovery and data mining, Association for Computing Machinery, New York, NY, USA, 24–28 July 2010; pp. 1039–1048.
22. Smutnicki, C.; Bożejko, W. Tabu search and solution space analyses. The job shop case. In *International Conference on Computer Aided Systems Theory*; Springer: Cham, Switzerland, 2017; pp. 383–391.
23. Yang, Q.; Chen, W.N.; Yu, Z.; Gu, T.; Li, Y.; Zhang, H.; Zhang, J. Adaptive multimodal continuous ant colony optimization. *IEEE Trans. Evol. Comput.* **2016**, *21*, 191–205. [[CrossRef](#)]
24. Wang, D.; Tan, D.; Liu, L. Particle swarm optimization algorithm: an overview. *Soft Comput.* **2018**, *22*, 387–408. [[CrossRef](#)]
25. Kennedy, J.; Eberhart, R. Particle swarm optimization. In Proceedings of the ICNN'95-International Conference on Neural Networks, IEEE, Perth, WA, Australia, 27 November–1 December 1995; Volume 4, pp. 1942–1948.
26. Poli, R.; Kennedy, J.; Blackwell, T. Particle swarm optimization. *Swarm Intell.* **2007**, *1*, 33–57. [[CrossRef](#)]



© 2020 by the authors. Licensee MDPI, Basel, Switzerland. This article is an open access article distributed under the terms and conditions of the Creative Commons Attribution (CC BY) license (<http://creativecommons.org/licenses/by/4.0/>).